Interactions of bound excitons in doped core/shell quantum dot heterostructures

Assaf Avidan, Zvicka Deutsch, and Dan Oron
Department of Physics of Complex Systems, Weizmann Institute of Science, Rehovot 76100, Israel
(Received 12 April 2010; revised manuscript received 20 July 2010; published 27 October 2010)

Spatial localization to a defect or a dopant of one of the charge carriers comprising an exciton, has a significant effect on the optical properties of bulk semiconductors. It is not clear, however, how these effects would change when considering semiconductor nanocrystals in the strong confinement regime. As we show here, under strong confinement, doping has a dramatic effect on the energetics of multiply excited states, which exhibit a strong size dependence. This is experimentally shown by performing multiexciton spectroscopy of CdSe/CdS and ZnSe/CdS colloidal quantum dot (QD) heterostructures, whose cores are nucleation-doped with few atoms of tellurium, leading to localization of the holes. The biexciton (BX) is shown to be strongly blueshifted relative to the bound exciton, in stark contrast with the corresponding undoped nanocrystals exhibiting a BX redshift. The energetics of the BX is shown to be determined mostly by the energy difference between the dopant state and the valence-band edge while the emission color is mostly determined by quantum confinement in the conduction band. By tailoring the nanocrystal's structure we can thus independently control the emission color, the radiative decay rate and the BX repulsion. QD heterostructures harboring bound excitons are therefore excellent candidates for colloidal-based gain devices required to operate in the single exciton gain regime.

DOI: 10.1103/PhysRevB.82.165332 PACS number(s): 78.67.Hc, 78.47.jd, 73.90.+f

A bound exciton (X) is formed in a semiconductor when one of the charges, either the electron or the hole, is spatially localized to a dopant or a defect.[1] Bound excitons have been extensively studied in bulk semiconductors since they frequently appear in the emission and absorption spectra of bulk crystals. Impurities or dopant centers exist in semiconductors either in cases where the crystal is considered to be "pure" (meaning low-impurity concentration[2–4]), or are inserted deliberately for enhanced emission (see, for example, Refs. 5–8, for the work done on tellurium-doped CdS and ZnS). Since the electrical and chemical nature of such impurity centers are mostly unknown, much of the effort has been invested in trying to determine whether the excitons are electrically bound to a neutral dopant center or to a charged donor or acceptor, as well as providing chemical and geometrical characterization. Bound exciton luminescence is also observed from indirect-gap semiconductors such as silicon or GaP,[9–12] where optical transitions are possible only because the doping atoms break the translational symmetry of the crystal. In direct gap materials, excitons bound to impurities can create energy defect states within the gap which cause a Stokes shift of the emission. This work focuses on one of the most studied such systems: that of II-VI semiconductors [such as CdS,[5] ZnS,[8] or ZnSe (Ref. 15)] which are isovalently doped by tellurium. In these materials and their corresponding alloys, the optical properties of the tellurium defects have been shown to be strongly dependent on the number of clustered tellurium atoms comprising it. Where in ZnS a single tellurium atom is sufficient to create large binding energies[14] (several 100 meV), in ZnSe tellurium doublets are necessary for bound excitons (with 100 meV binding energy) to appear.[13]

It is interesting to consider the analogy between bulk bound excitons and bound excitons in quantum dots (QDs) in the strong confinement regime. One clear consequence of quantum confinement is an energetic shift of the band edge. Thus, dopants are expected to localize charge carriers in QDs more easily than in the bulk case. It should be considered, however, that even in undoped QDs, both charge carriers are essentially localized to the nanocrystal, so the very meaning of a bound exciton requires some reformulation. Since the total number of atoms in one colloidal QD is very small compared to bulk materials (ranging between several hundreds to few thousands), a QD is doped when only a few of the host atoms are replaced by dopant ones. Thus, upon a weak optical excitation, either the electron or hole or both are inevitably localized to a dopant site. In practice the dopant can be incorporated either via nucleation doping (that is, the host nanocrystal growth is initiated by a small cluster of dopant atoms), or via growth doping (whereby dopant atoms are incorporated into the nanocrystal during the growth phase). While the former results in a single dopant nucleus (a cluster of a few atoms), in the latter, dopant atoms are not all localized to adjacent lattice sites.[16] Some recent examples of successful doping of II-VI colloidal nanocrystals include Mn-doped ZnSe,[17,18] and Cu-doped ZnSe,[16] (for a complete review see Ref. 19). Under a weak optical excitation, doped colloidal QDs exhibit rather similar optical behavior to doped bulk semiconductors, in particular a redshifted emission wavelength relative to the QD band edge, and modified radiative decay dynamics. In cases where only one charge carrier is localized to the dopant, such as ZnSe:Cu QDs,[16] the emission color is also size dependent due to the quantum confinement energy of the delocalized carrier.

Since defect states in colloidal QDs are not spatially resolved as in dilute bulk samples, differentiating between the presence of a single dopant site and multiple dopant sites from simple optical measurements is an extremely difficult task. However, charge localization does have a strong effect on the X-X interaction energies in quantum confined systems [the terms X-X and biexciton (BX) are used to describe two excitons excited in the same dot]. The nature of the X-X interaction depends on the band alignment of QD heterostructures. In Type I QDs both charge carriers are localized

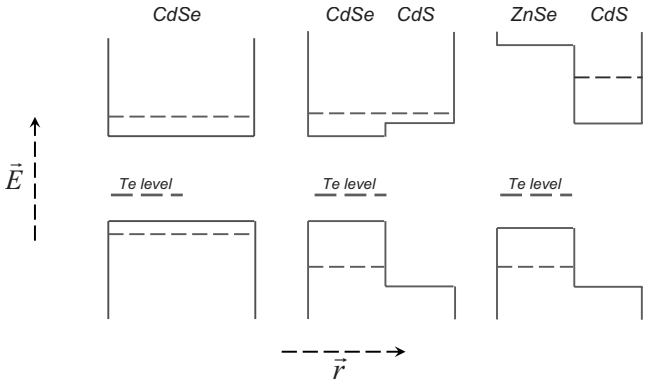

FIG. 1. The Energy diagrams for type I configuration CdSe:Te, quasitype II CdSe:Te/CdS, and type II ZnSe:Te/CdS are shown. The ground-state energy for the electron and hole in each structure is plotted by a dashed line, along with the tellurium defect state, which is at the same energetic position for all three configurations. Note that due to the confinement effect of the CdS, the hole ground state of the CdSe:Te QDs is higher than for the CdSe:Te/CdS QDs.

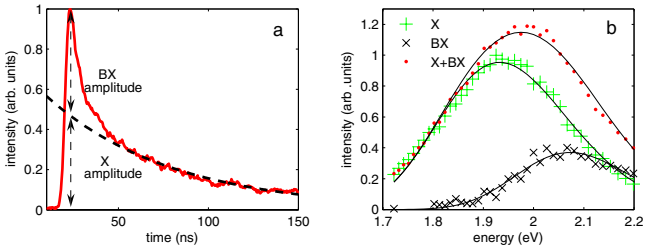

FIG. 2. (Color online) X and BX decomposition procedure. Here we used a CdSe:Te/CdS sample with a core with emission centered around 570 nm. Several monolayers of CdS where grown and the emission of the final sample is at 640 nm (1.9 meV as can be seen in b). The spectrum is taken at a power which is high enough to show BXs but still low enough to prevent the appearance of *triexcitons*. (a) Transient taken at ~8 *ph/dot/pulse*. The long exponential tail (dashed black) splits the fast and slow amplitudes which are then plotted as a function of the photon energy. (b) The amplitude of the slow (green pluses) and fast (black ×-marks) are plotted, along with their sum shown in red dots.

either to the core or to the shell, resulting in a negative (binding) X-X interaction energy.[20] In type II core-shell QD heterostructures, one charge carrier is localized to the core and the other is either delocalized (quasitype-II), or localized to the shell. As a result, in colloidal QDs the X-X interaction can be tuned from attractive to repulsive,[21,22] by varying the relative thickness of the core and shell layers. Recently we have shown[23] that nucleation-doped CdSe:Te nanocrystals also exhibit a large BX repulsion of up to 300 meV. However, unlike type II QDs the X-X interaction energy in CdSe:Te QDs decreases with size. This behavior suggests a different regime of the X-X interaction. Such systems, exhibiting strong X-X interactions are of great interest, particularly in the context of optical amplification, where optical gain in the single exciton regime is desired.[24,25]

In the following study we investigate X-X interactions of bound excitons in two different heterostructures with nucleation-doped cores: CdSe:Te/CdS QDs and ZnSe:Te/CdS QDs. We show that in both cases, nucleation doping of tellurium indeed results in a strong repulsive X-X interaction. We directly compare the X-X interaction in both the doped and undoped QDs and clearly show that this behavior is solely due to the presence of tellurium dopant atoms. We thus generalize the results presented in Ref. 23, and claim that doped QDs form a unique class of QDs, different from type I and type II systems. In contrast to type I and type II systems, excitons in nucleation-doped QDs are bound, and as a result they strongly repel each other with energies that scale with the Stokes shift of the emission. The results are qualitatively explained by an effective mass model whereby an isolated defect state within the QD is taken into account by a potential well with a fixed radius. Finally, implications on the design of high-quantum-yield QDs for optical gain applications are considered.

The band diagrams for the experimentally studied systems are shown schematically in Fig. 1, and plotted in such a way that the tellurium energy level is the same in all three diagrams. In the first part of this paper we examine the effect of a CdS shell growth on CdSe:Te QDs. Growth of a CdS shell enables us to separately control the effect of the valence and conduction band on the X-X interaction energy. While the electron extends over the entire CdSe:Te/CdS QD, the CdS shell localizes the hole in the doped CdSe core. In the second part of the paper we show the generality of the doped regime by introducing a new system, ZnSe:Te/CdS, which has a type II band alignment. This system shows a very similar behavior to that of CdSe:Te/CdS despite the different material composition.

We excite a dilute QD solution with a Q-switched 355 system that produces 5 ns pulses at 10 Hz. The QDs fluorescence is collected using a high numerical aperture lens, spectrally filtered by a monochromator, and detected with a fast photo multiplier tube and a digital oscilloscope. Figure 2 shows the procedure used to extract the X-X interaction term. In the figure we show a decay curve taken at a high photon fluence, at the peak of the BX emission [2.1 eV in Fig. 2(b)]. Because of the short Auger lifetime associated with the BX decay in QDs in the strong confinement regime, the exciton and BX decays are completely separated in time. The decay is split between a fast decay with the system response time constant (~10 ns), and a long exponential tail of about ~100 ns (fitted to the data). Following the analysis presented in Ref. 21, we found an Auger lifetime which is roughly 10–100 ps. Such a short lifetime cannot arise from modification of the exciton radiative rate due to, for example, band bending.

The relative amplitudes of the two components are then plotted to obtain their spectrum.[20,21] Figure 3(a) shows the previously published data[23] of X-X repulsion of CdSe:Te (blue diamonds), and on top the results obtained by growing a new CdSe:Te core (left red triangle), and over coating it with a CdS layer (other two red triangles). The CdS shell growth results in a redshift of the emission due to electron delocalization into the CdS shell. The X-X repulsion energy is, however, significantly larger than in the core only case, despite the fact that the CdSe:Te/CdS QDs are actually larger than their CdSe:Te counterparts emitting at the same wavelength. Up to an emission wavelength of 640 nm the blue-

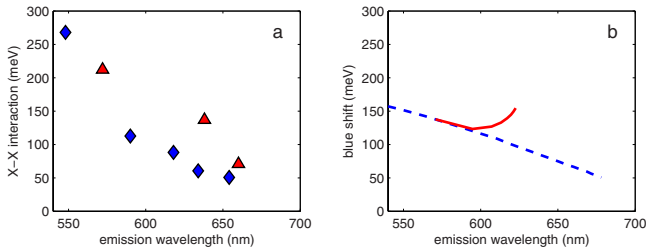

FIG. 3. (Color online) X-X interaction energies for the CdSe:Te QDs with an over grown shell of CdS. The blue dots are of core only QDs. The first red dot (emission at 570 nm) is a core only QD which was over coated with CdS shell (other two red dots). (b) Effective mass calculation for the doped core and core/shell QDs. The results for the core only CdSe:Te are shown in dashed blue, and the red line is for the CdSe:Te/CdS core shell QDs.

shift (repulsive X-X interaction) is indeed high (between 100–150 meV), where above 640 nm it drops to around 50 meV. In order to provide a deeper understanding of the results presented above, we propose an effective mass three-dimensional toy model which treats the tellurium defect state by considering a deep hole trap potential within the CdSe host, supporting a single hole bound state. The trap has a fixed width (r_{trap}=0.25 nm, which matches the approximate size expected from a core of a few tellurium atoms), and depth of 3.3 eV, which is fixed to fit the X-X interaction data. Formally, our model is described by an effective mass Hamiltonian of two noninteracting electrons and two noninteracting holes, which are coupled by a Coulomb interaction term V_c added to each one of them. The Coulomb interaction term is given by

$$V_c(r) = \int_{-\infty}^{r} \frac{Q(r')}{\epsilon r'^2} dr', \tag{1}$$

where ϵ is the bulk dielectric const, $Q(R)$ is the total charge contained in a region of radius R. The total charge Q is related to the electron and hole wave functions by Gauss's law,

$$Q(r') = \int_{0}^{r'} e(|\Psi_e|^2 - |\Psi_h|^2) d^3x. \tag{2}$$

Here Ψ_e and Ψ_h are the wave functions of the electron and hole, respectively, which solve the total Hamiltonian, and e is the electron charge. The total Hamiltonian is given by

$$\left[-\frac{1}{2m_{e,h}} \left(\frac{2}{r}\partial_r + \partial_r^2 \right) + V_{e,h}(r) \mp V(r) \right] \Psi_{e,h} = E_{e,h} \Psi_{e,h}, \tag{3}$$

where $V_{e,h}$ is the confining potential of the semiconductor, $m_{e,h}$ is the effective mass of the electron/hole in the bulk, and the minus and plus signs are for electrons and holes, respectively. Since we are looking for the ground-state solution, we only consider the spherical part of the effective mass Hamiltonian with no angular dependence. Equation (3) presents a system of two coupled nonlinear equations which are solved

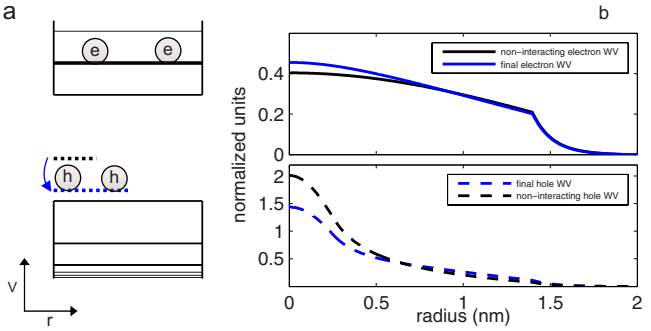

FIG. 4. (Color online) Comparison between the energies and the wave functions of electrons and holes with and without the interaction potential. The integrated modulus of all the wave functions equals unity (normalized units). a) As a result of the interaction term the hole energy level originally in the gap, is pushed down toward the band edge. (b) In the space domain the hole wave function with the interaction potential (dashed blue) is wider than the hole wave function without the interaction potential (dashed black). The electron wave function is hardly changed by the interaction potential.

iteratively and self-consistently until convergence of the eigenvalues is achieved. Denoting by $E^o_{e,h}$ the solution without the interaction potential $V(r)$, the X-X interaction term is then defined by

$$E_{xx} = (E^o_e + E^o_h - E^o_{eh}) - (E_e + E_h - E_{eh}), \tag{4}$$

where E_{eh} is the electron-hole Coulomb attraction term calculated following Ref. 26. The blue dotted lines in Fig. 3(b) show the results for CdSe without a CdS shell. Although the effective mass model is a crude approximation, it qualitatively recovers the trend of the X-X interaction energy, which decreases with the size of the dot. Figure 4(a) sketches the energy levels of the hole, with (dashed blue) and without (dashed black) the interaction potential. Since the interaction is repulsive for the hole, the solution (hole energy level) converges to a level closer to the band edge, reducing the X-X interaction term. In the space domain, this results in a wider wave function only for the hole [see Fig. 4(b)] while the electron wave function is hardly affected by the interaction.

We also examined the results of our model for the case of the core-doped CdSe:Te/CdS heterostructure (red line). In this case the confinement of the hole is maintained because of the large offset between the CdS and the CdSe valence bands but the electron is relatively delocalized. This leads to an increased X-X repulsion for QDs with a thick CdS shell, similar to the case of type II QDs. While the experimental results show an increased repulsion for QDs with a thick CdS shell (relative to the CdSe QDs emitting at the same color), the X-X interaction energy still decreases with size. Note also that the maximum emission wavelength of the doped CdSe/CdS QDs in the model is 640 nm while the experimental value is as high as 650 nm or more. This suggests that alloying between the CdSe and CdS layers may have occurred. Such chemical modifications and in particular dopant diffusion which results in a weaker binding potential,

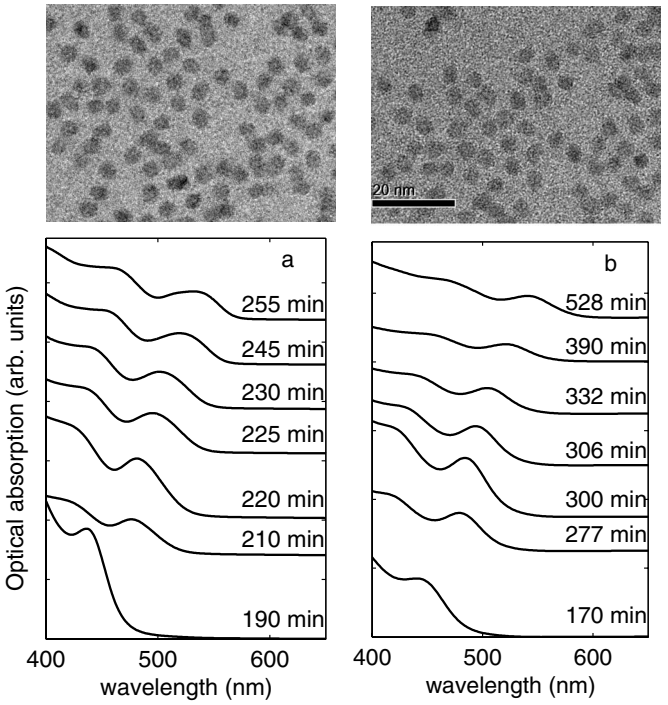

FIG. 5. Absorption spectra taken during the synthesis of (a) undoped ZnSe/CdS QDs and (b) ZnSe:Te/CdS QDs. The spectra at different times are shifted upwards for clarity. Above each plot we show TEM images that correspond to the final stages of the growth procedure.

might also explain the disagreement between the measurement and the calculation since diffusion of tellurium atoms from the core results in a reduced binding potential for the holes.[15]

Next we would like to show that the behavior we observe in doped CdSe/CdS QDs is more general and is applicable to other materials as well. Thus, we extend this idea to type II ZnSe/CdS QDs. We developed a synthetic route for producing ZnSe:Te cores, in which we use known methods with slight modifications.[27] These are then overcoated by a CdS shell. Our synthesis produces spherical shaped and very bright core/shell QDs with a high (~50%) quantum yield [see transmission electron microscope (TEM) images in Fig. 5]. Detailed description of the synthesis can be found in the supporting information. In addition, a reference undoped system of ZnSe/CdS QDs was also synthesized for direct comparison.

In Fig. 5 we show the absorption spectra of regular QDs ZnSe/CdS [Fig. 5(a)] and of the ZnSe:Te/CdS QDs [Fig. 5(b)], taken with a UV-Visible spectrophotometer. The core sizes in both cases are the same (absorption peak at 370, not shown), and the evolution of the absorption spectrum during the CdS growth is very similar. However, the emission of the doped particles seems red shifted [Fig. 6(b)] and much broader, which is very similar to the emission pattern obtained for CdSe:Te (see Refs. 23 and 28). Since the size distribution of the doped and undoped ZnSe/CdS QDs is approximately the same (see Fig. 5), the broad emission profile of the doped particles is not the result of a broad size distribution. However, small changes in the number of Tellurium atoms incorporated in each dot can shift the emission peak wavelengths. We believe that like in the case of CdSe:Te, the redshifted emission here results from a hole trap state inside the ZnSe gap, and its broadening is the result of the tellurium atom number distribution.

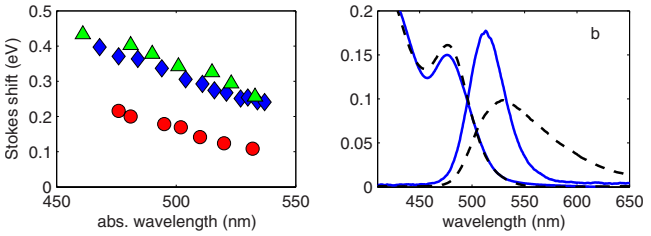

FIG. 6. (Color online) (a) Stokes shift as a function of the absorption wavelength for the ZnSe/CdS (red circles) QDs, ZnSe:Te/CdS (blue diamonds) QDs, and for ZnSe:Te/CdS QDs (green triangles) made from a smaller ZnSe:Te core. (b) Absorption and emission of the ZnSe/CdS QDs (blue line), and of the ZnSe:Te/CdS QDs (black dashed line). Note the smaller overlap between the absorption and emission spectra of the doped particles.

Because of the asymmetry in the emission profile of the ZnSe:Te/CdS QDs, we define the Stokes shift as the distance between the first absorption maximum and the emission centroid. The Stokes shift of the ZnSe/CdS (red circles) and the ZnSe:Te/CdS (blue diamonds) QDs is directly compared in Fig. 6(a) as a function of the absorption wavelength, where we also show the Stokes shift of ZnSe:Te/CdS QDs made from a smaller core (absorption 355 nm shown in green triangles). We find that the Stokes shift is substantially higher (about 150 meV) for the ZnSe:Te/CdS, which is a clear sign of tellurium related emission.[23,28] We also find that for a smaller ZnSe:Te core, the Stokes shift is slightly higher. This is consistent with an energy trap state located deeper inside the host energy gap, attributed to the larger valence-band confinement energy. In addition to a larger Stokes shift, we also measured an exciton lifetime three times longer for the doped QDs (~60–80 ns), and even longer lifetimes (~80–100 ns) for ZnSe:Te/CdS QDs made from a smaller core (see supporting info). The above measurements show the same qualitative behavior that was observed for CdSe:Te QDs, from which we infer that the majority of our dots contain tellurium atoms. However, the exact number distribution of the tellurium atoms incorporated into the dots and their specific geometry is unknown and requires further study. Such a mechanism of hole trapping which shows resemblance to the CdSe:Te QDs, suggests that a strong X-X repulsion should be revealed in our measurements.

In Fig. 7(a) we plot the X-X interaction energy as a function of the emission wavelength, where negative values stand for binding X-X interaction. In red circles and blue diamonds we show the results for ZnSe/CdS and ZnSe:Te/CdS, respectively, for which the initial core size is the same. The doped particles show X-X repulsion energies whereas the ZnSe/CdS QDs show binding. Such binding energies are unexpected for a type II system, and possibly indicate the existence of an alloyed layer of CdSe in the ZnSe-CdS interface, somewhat localizing both electrons and holes. Moreover, it appears that the X-X interaction in the ZnSe:Te/CdS particles

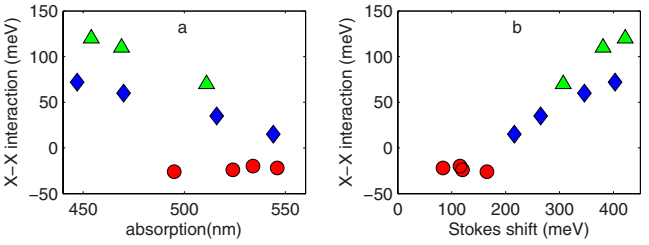

FIG. 7. (Color online) (a) X-X energies of the ZnSe/CdS QDs (red circles), ZnSe:Te/CdS made from a core with the same size as that of the undoped QDs (blue diamonds), and ZnSe:Te/CdS made from a smaller core size (green triangles). (b) The same X-X interaction energies as in (a) plotted against the Stokes shift.

depends on the thickness of the CdS shell, where it is clear that for the ZnSe/CdS QDs it is almost constant. The dots with the smaller core [green triangles in Figs. 7(a) and 7(b)] show the same behavior only with a larger X-X repulsion that reaches a value as large as 130 meV across a broad tuning range, a task which is unachievable with undoped QDs.[29] This is consistent with our understanding as described above. A smaller core suggests that the tellurium defect state is located deeper in the gap and induces a larger spatial confinement to the hole. This leads to a larger Coulomb repulsion between the two holes upon a double excitation.

Measurements of the X-X interaction energy in the core only particles in both the doped and undoped cases (ZnSe and ZnSe:Te) were impossible due to their low-quantum yield. However, since smaller cores exhibit stronger interactions, it is likely that the X-X interaction energy dependence on size in these dots obey the same trend as in the CdSe:Te QDs. More insight into the problem is obtained by considering the X-X interaction energy as a function of the emission Stokes shift. Since a deeper defect induces a larger repulsion, we expect the interaction energy to increase as a function of the Stokes shift. In Fig. 7(b) we plot the X-X repulsion energy as a function of the Stokes shift, for the ZnSe/CdS QDs (red circles), the core size compatible ZnSe:Te/CdS QDs (blue diamonds), and for the smaller core doped particles (green triangles). The difference between the doped and undoped QDs is obvious. Indeed, the X-X interaction energy of the ZnSe:Te/CdS QDs has a linear dependence on the Stokes shift whereas the X-X interaction energy of the ZnSe/CdS (red circles) QDs does not depend on the Stokes shift at all. These findings confirm the existence of a doped regime in which the X-X interaction is primarily set by the degree of hole localization, and thus directly proportional to the Stokes shifted emission. This is in contrast to the type II regime where the X-X interaction is determined by electron/hole charge separation.

To conclude, we performed quasi-continuous-wave spectroscopy on colloidal CdSe:Te/CdS and ZnSe:Te/CdS QDs. We showed the generality of a doped regime in which the X-X interactions are repulsive and are dominated by the spatial localization of the holes on the defect state, and scale with the emission Stokes shifted spectrum of the dot. A simple description of this regime is facilitated by considering the following: Two holes cannot be localized to the defect due to a strong Coulomb repulsion. On the other hand, from studies of type-I QDs,[20] it is known that the X-X interaction is attractive if the two holes become completely delocalized. Hence, the BX state lies between the (constant) energetic position of the defect and the first delocalized hole state, whose energy decreases with size. This leads therefore to a weaker repulsion at larger sizes.

In the case of CdSe:Te/CdS QDs, we have found that the CdS shell indeed increases the X-X interaction energies compared to CdSe:Te cores with the same emission wavelength. This provides tunability over part of the visible (~550–640 nm) with X-X interaction energies ranging between 200–100 meV. For ZnSe:Te/CdS, we showed that it reveals the same qualitative behavior as the CdSe system. Namely, a larger Stokes shift, broader emission spectra, longer lifetimes, and most importantly, a repulsive X-X interaction above 100 meV in dots with emission between 500–550 nm. We believe that the results presented here are general. In particular they do not depend on the specific material composition and band alignment of doped QDs with a single defect state, as is readily achieved by nucleation doping. The Stokes shift and the X-X interaction energy are closely linked, and to our understanding both originate from a deep hole trap in the gap of the host. Such a regime is unique and is completely different from type-I and type-II heterostructures, opening new possibilities of band gap engineering of quantum confined systems. We have achieved a relatively large X-X repulsion of over 100 meV over a large part of the visible range, which is desirable in the context of gain applications. We believe these ideas can be readily extended to systems which emit in the near-infrared spectral range, and that stronger repulsion can be obtained by using different dopants inducing states deeper within the host gap. In this context, ZnSe:Cu and CdSe:Cu QDs, as well as PbSe:Te and PbS:Te seem to be promising candidates.

We would like to thank Stella Itzhakov for quantum yield measurements and Ronit Popovitz-Biro for her help with TEM imaging. This research was supported by the Israeli ministry of science culture and sport, by the ministry of research of Korea and by the Minerva foundation, with funding from the Federal German ministry of education and research. Transmission electron microscopy studies were conducted at the Irving and Cherna Moskowitz Center for Nano and Bio-Nano Imaging at the Weizmann Institute of Science.

[1] Y. Y. Peter and M. Cordona, *Fundamentals of Semiconductor, Physics and Material Properties* (Springer, New York, 1983), Chap. 7.
[2] D. J. Thomas and J. J. Hopfield, Phys. Rev. **128**, 2135 (1962).
[3] J. J. Hopfield, D. J. Thomas, and R. T. Lynch, Phys. Rev. Lett. **17**, 312 (1966).
[4] R. E. Dietz, D. J. Thomas, and J. J. Hopfield, Phys. Rev. Lett. **8**, 391 (1962).
[5] A. C. Aten and J. H. Haanstra, Phys. Lett. **11**, 97 (1964).
[6] J. D. Cuthbert and D. J. Thomas, J. Appl. Phys. **39**, 1573 (1968).
[7] D. M. Roessler, J. Appl. Phys. **41**, 4589 (1970).
[8] T. Fukushima and S. Shionoya, Jpn. J. Appl. Phys. **12**, 549 (1973).
[9] D. J. Thomas, J. J. Hopfield, and C. J. Frosch, Phys. Rev. Lett. **15**, 857 (1965).
[10] D. J. Thomas and J. J. Hopfield, Phys. Rev. **150**, 680 (1966).
[11] J. D. Cuthbert and D. G. Thomas, Phys. Rev. **154**, 763 (1967).
[12] J. R. Haynes, Phys. Rev. Lett. **4**, 361 (1960).
[13] A. Muller, P. Bianucci, C. Piermarocchi, M. Fornari, I. C. Robin, R. Andre, and C. K. Shih, Phys. Rev. B **73**, 081306 (2006).
[14] K. P. Tchakpele, J. P. Albert, and C. Gout, J. Cryst. Growth **72**, 151 (1985).
[15] D. Lee, A. Mysyrowicz, A. V. Nurmikko, and B. J. Fitzpatrick, Phys. Rev. Lett. **58**, 1475 (1987).
[16] N. Pradhan, D. Goorskey, J. Thessing, and X. Peng, J. Am. Chem. Soc. **127**, 17586 (2005).
[17] N. Pradhan and X. Peng, J. Am. Chem. Soc. **129**, 11 (2007).
[18] D. J. Norris, N. Yao, F. T. Charnock, and T. A. Kennedy, Nano Lett. **1**, 3 (2001).
[19] D. J. Norris, A. L. Efros, and S. C. Erwin, Science **319**, 1776 (2008).
[20] D. Oron, M. Kazes, I. Shweky, and U. Banin, Phys. Rev. B **74**, 115333 (2006).
[21] D. Oron, M. Kazes, and U. Banin, Phys. Rev. B **75**, 035330 (2007).
[22] A. Sitt, F. Della Sala, G. Menagen, and U. Banin, Nano Lett. **9**, 3470 (2009).
[23] A. Avidan and D. Oron, Nano Lett. **8**, 2384 (2008).
[24] V. I. Klimov, A. A. Mikhailovsky, S. Xu, A. Malko, J. A. Hollingsworth, C. A. Leatherdale, H. J. Eisler, and M. G. Bawendi, Science **290**, 314 (2000).
[25] V. I. Klimov, S. A. Ivanov, J. Nanda, M. Achermann, I. Bezel, J. A. McGuire, and A. Piryatinski, Nature (London) **447**, 441 (2007).
[26] D. Schooss, A. Mews, A. Eychmuller, and H. Weller, Phys. Rev. B **49**, 17072 (1994).
[27] See supplementary material at http://link.aps.org/supplemental/10.1103/PhysRevB.82.165332 for a detailed description. In short, the synthesis is done in a one-pot approach. In the synthesis of ZnSe:Te cores, 5% of the selenium content is replaced with tellurium, and is injected to a hot mixture of ODE and HDA. For the growth of a CdS shell we use $Cd(Ol)_2$ and sulphur in ODE.
[28] T. Franzl, J. Müller, T. A. Klar, A. L. Rogach, J. Feldmann, D. V. Talapin, and H. J. Weller, PhysChemComm **111**, 2974 (2007).
[29] A. Piryatinski, S. A. Ivanov, S. Tretiak, and V. I. Klimov, Nano Lett. **7**, 108 (2007).